UPFC Based on Improved Double-loop Decoupling by comparing PI & Fuzzy Control in Photovoltaic Systems

Mr. M. Kiran
Student, Dept of EEE, Teegala Krishna Reddy Engineering College/JNTUH, Hyderabad, A.P, INDIA

Abstract -**The mutation of solar irradiance can cause the output power of photovoltaic power plant to mutate, and it takes great changes to active power and reactive power which feed into the power grid. When the system security constraint is exceeded, the photovoltaic power plant will stop running. In this project, the structure and the mathematical model of large grid-connected photovoltaic power plant are introduced; then an improved double loop decoupling by comparing PI & Fuzzy control system is proposed based on the d-q model of UPFC parallel converter. On the basis of traditional PI & Fuzzy control, DC load current is directly used as feed-forward control in the control system of capacitor voltage. It is not only easy to get feedback, but also conducive to design and operate the series controller and the parallel controller independently. Finally, this paper sets up a Simulink model of UPFC in the environment of Matlab/Simulink after analyzing its principle. And then, this model was applied into a three-phase system to observe its influences to power quality. The simulation results show that this PI & Fuzzy control system based on the UPFC can effectively control the voltage and the power flow, maintain bus voltage and reduce reactive exchange. It can also improve the active photovoltaic power transmission, as well as maintaining the stability of the system.**

Keywords: Photovoltaic power system, Unified power flow controller (UPFC), power flow analyze, PI controller and Fuzzy logic controller (FLC).

1. INTRODUCTION

The word "photovoltaic" consists of two words: photo, a greek word for light, and voltaic, which defines the measurement value by which the activity of the electric field is expressed, i.e. the difference of potentials. Photovoltaic systems use cells to convert sunlight into electricity. Converting solar energy into electricity in a photovoltaic installation is the most known way of using solar energy. Now a days the production, which reached a large scale, the whole industry production of solar cells has been developed and, due to low production cost, it is mostly located in the Far East. Photovoltaic cells produced by the majority of today's most large producers are mainly made of crystalline silicon as semiconductor material. Large grid-connected photovoltaic power plant is an important developing direction of photovoltaic power generation. Because the PV power plant's generating capacity varies with temperature, irradiance and other changes, when it is in the larger proportion of the grid, the intermittent and abrupt will cause the fluctuations and changes of power flow. So, the difficulty of voltage adjustment in the power grid is increased. In severe cases, it may play a destructive role on the voltage at access point and even the whole power grid [1].

Flexible AC Transmission Systems (FACTS) technology is the ultimate tool for getting the most out of existing equipment via faster control action and new capabilities. The most striking feature is the ability to directly control transmission line flows by structurally changing parameters of the grid, and to implement high-gain type controllers based on fast switching [2]. The UPFC is the most versatile FACTS device that has emerged for the control and optimization of power flow in electrical power transmission systems [5]-[6]. It offers major potential advantages for the static and dynamic operation of transmission lines since it combines the features of both the Static Synchronous Compensator (STATCOM) and the Static Synchronous Series Compensator (SSSC). UPFC can control both active and reactive power flows, as well as amplitude and phase of the line node voltage. With the emergence of a number of megawatt-class centralized PV power plants, it is the direction of extensive research in order to further the development of photovoltaic power generation [8]-[9]. UPFC based on the double loop decoupling by comparing pi and fuzzy control on the basis of traditional fuzzy logic provides a general concept for description and measurement. Fuzzy logic comprises fuzzy sets, which are a way of representing non-statistical uncertainty and approximate reasoning, which includes the operations used to make inferences in fuzzy logic [10]-[15]. This paper sets up a Simulink model of UPFC in Matlab/Simulink by comparing PI and Fuzzy control model of PV power plant system active, reactive power and bus voltage are improved. this model was applied into a three-phase system to observe its influences to power quality. Benefits of using UPFC will be presented by simulation results.

The performance of the proposed system is demonstrated through simulated waveforms using Sim Power Systems (SPS) Matlab/Simulink environment. Composition and modeling of grid- connected photovoltaic power plant discussed in Section 2, System structure and the mathematical model of UPFC is illustrated in Section 3 and the comparison of PI and Fuzzy logic controller

IJERT

explained in section 4. The SPS Matlab/Simulink-based simulation results are explained in Section 5. Section 6 concludes the paper.

2. COMPOSITION AND MODELING OF GRID-CONNECTED PHOTOVOLTAIC POWER PLANT

Grid-connected photovoltaic power station mainly consists of photovoltaic array, inverter with maximum power point trace (MPPT), filter capacity, filer inductance, transformer and control system etc. The differences between grid-connected photovoltaic power station and traditional power supply lie in: special output IV characteristics of photovoltaic array, MPPT function, oriented vector control of voltage, and random city of output electrical power. In order to simulate more accurately these characteristics, the ideas of controlled current source and controlled voltage source are introduced; when the requirements for the balance of instantaneous power are met, the figures of equivalent circuit can be derived. Among the following figures, Fig.1(a) is the equivalent circuit from photovoltaic array to the outlet end of inverter, Fig.1(b) is the equivalent circuit from the outlet end of inverter to transformer, and Fig.1(c) is the equivalent circuit from the outlet end of transformer to grid-connecting node [2].

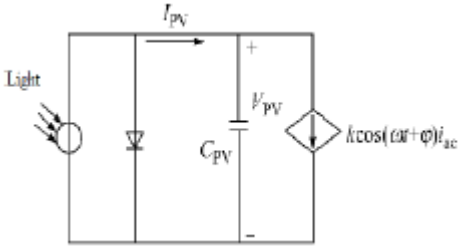

(a) From photovoltaic array to inverter

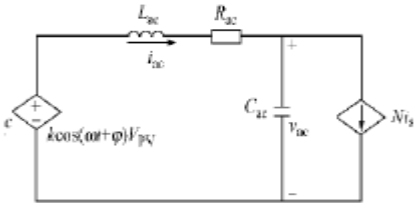

(b) From inverter to transformer

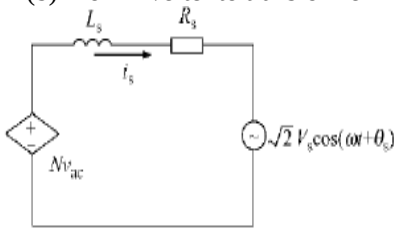

(c) From transformer to grid-connecting node

Fig.1 Equivalent circuit diagram of the PV power plant

A current equation, Formula (1), can be derived by KCL from Fig. 1 (a)

$$I_{PV} - C_{PV}\frac{dV_{PV}}{dt} - ki_{ac}\cos(\omega t + \varphi) = 0 \quad (1)$$

where, k is the modulation depth of inverter is the phase angle of the modulation of inverter, and both of them are the control parameters of inverter.ω is power frequency angular velocity, and the meanings of other physical quantities are the same as those in Fig.1. The output current *PV I* and terminal voltage *PV V* of photovoltaic array can be characterized by Formula (2) [4].

$$\begin{cases} I_{PV} = N_P N_{P1} I_L - N_P N_{P1} I_0 \left[e^{\frac{qV_{PV}}{nKTN_{s1}N_s}} - 1 \right] \\ V_{PV} = \dfrac{N_{S1} N_S nKT}{q} \ln\left[\dfrac{N_{P1} N_P I_L - I_{PV}}{N_{P1} N_P I_0} + 1 \right] \\ P_{pv} = \max\left(I_{PV} V_{PV}\right)\Big|_{I_L, T} \end{cases} \quad (2)$$

In this formula, 1 and *P P N N* represent the parallel number of photovoltaic array and photovoltaic module respectively; 0 *I* is saturation current; *n* is factor, also named as diode quality factor, which can be set as 1.2 if photovoltaic components are made of crystalline silicon or can be set only after evaluation if photovoltaic components are made of amorphous silicon; *q* is charging electric charge quantity, commonly 1.60*e*−19; *K* is Boltzmann constant, commonly 1.38*e*−23 ;*T is* temperature(K), which is 298k under standard test temperature; *S N* and *S*1 *N* represent the serial number of photovoltaic array and photovoltaic module respectively; *PV P* is the output DC power (W) of the photovoltaic array of photovoltaic power station with MPPT [5]; *r I* is irradiation rate, which is the ratio between the irradiation and standard irradiation (1000*W* / *m*2). Formula (2) expresses the non-linear relation between the output current and the output voltage of photovoltaic array under any irradiation and module temperature. In Fig.2, (a) is I-V characteristics curve, and (b) is P-V characteristic curve

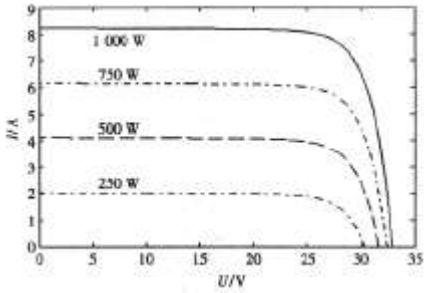

(a) I-V characteristics curve

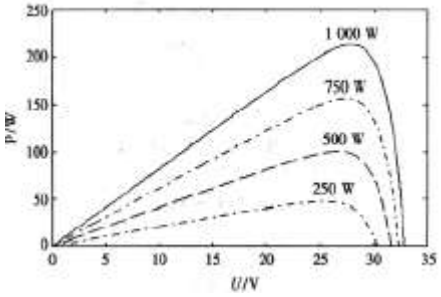

(b) P-V characteristic curve

Fig.2 I-V Characteristics curve and P-V characteristic curve of Photovoltaic array

A current equation and a voltage equation can be derived by KCL and KVL from Fig.1(b), see Formula (3) and (4):

IJERT

$$L_{ac}\frac{di_{ac}}{dt}+i_{ac}R_{ac}+v_{ac}=kV_{PV}\cos(\omega t+\varphi) \quad (3)$$

$$C_{ac}\frac{dv_{ac}}{dt}+Ni_s=i_{ac} \quad (4)$$

A voltage equation can be derived by KCL from Fig. 1 (c), see Formula (5):

$$L_S\frac{di_s}{dt}+R_Si_S+\sqrt{2}V_S\cos(\omega t+\theta)=Nv_{ac} \quad (5)$$

Non-linear time-varying equations (1) to (5) characterize the dynamic characteristics of grid-connected photovoltaic power station, and a vector function (6) can be derived by defining state [*X=Vpv,iac,vac,is*] and handling the equation set.

$$\dot{X}=f(\bar{X},t) \quad (6)$$

Vector function (14) depicts the dynamic characteristics of grid-connected photovoltaic power station and characterizes the mathematic model of it. According to the characteristics of the operation of grid-connected photovoltaic power station, simplified handling and solving can be made to this mathematical model, thus realizing the effective simulation of the operating mode [5]. Given that the AC quantities of grid-connected photovoltaic power generation system only include fundamental component, that is, all are standard sinusoidal quantities, which can be represented to be

$$i_{ac}=\sqrt{2}I_{ac}\cos(\omega t+\alpha)$$
$$v_{ac}=\sqrt{2}V_{ac}\cos(\omega t+\beta)$$
$$i_s=\sqrt{2}I_s\cos(\omega t+\theta)$$

and after they are substituted in Formula (1) to (5), an equation with vector can be derived as follows [7]:

$$I_{PV}-C_{PV}\frac{dV_{PV}}{dt}-\mathrm{Re}\left[\frac{k}{\sqrt{2}}\angle\varphi\right]\mathrm{Re}\dot{I}_{ac}=0 \quad (7)$$

$$\dot{I}_{ac}(R_{ac}+j\omega L_{ac})+\dot{V}_{ac}=\frac{kV_{PV}\angle\varphi}{\sqrt{2}} \quad (8)$$

$$j\omega C_{ac}\dot{V}_{ac}+N\dot{I}_s=\dot{I}_{ac} \quad (9)$$

$$(j\omega L_s+R_s)\dot{I}_s+\dot{V}_s=N\dot{V}_{ac} \quad (10)$$

Formula (7) actually represents the dynamic process of charging and discharging of the DC capacitor at the outlet end of photovoltaic array. Formula (8) to (10) represent the connecting relation of electric network of grid-connected photovoltaic power station. Formula (7) to (10) define the dynamic mathematical model of grid-connected photovoltaic power station given that AC quantities only concern fundamental component.

3. SYSTEM STRUCTURE AND THE MATHEMATICAL MODEL OF UPFC

3.1 Basic structure of UPFC

The system structure of UPFC is shown in Fig.3. It's core structure is two three-phase PWM inverters. The parallel converter is connected to the grid through the parallel transformer T1 while the serial converter is connected to the grid through the series transformer T2. The series converter supply the power grid with series voltage *U2* whose amplitude *U2* and phase α2 is variable. At the same time, it can regulate the power flow of transmission lines. The Parallel converter supply the incoming end with parallel voltage *U1* whose amplitude *U1* and phase α1 is variable. It can stable not only capacitor voltage *U*dc at DC side but also voltage at incoming end of UPFC. In addition, the parallel control system and the serial control system can be designed and work independently [8].

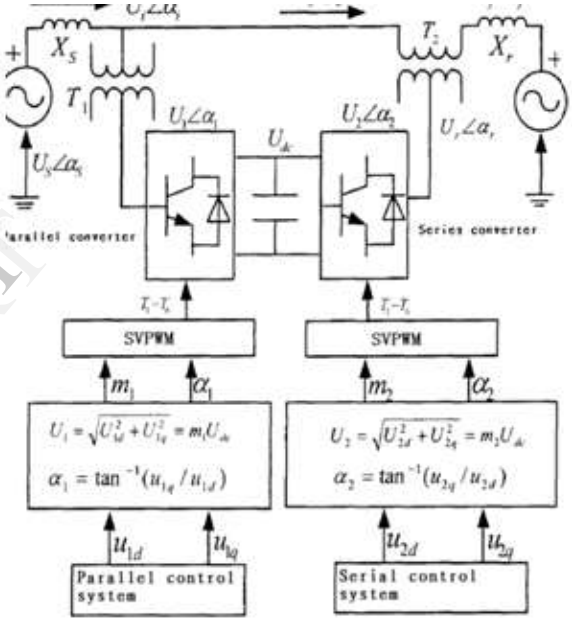

Fig.3 Basic structure of UPFC connected to power system

3.2 Design of shunt converter controller

The shunt converter circuit model UPFC is shown in Fig.4.

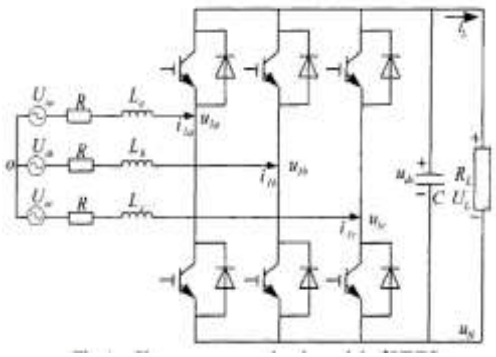

Fig.4 Shunt converter circuit model of UPFC

IJERT

The switching device in main circuit uses IGBT and anti-parallel diode. It is regarded as an ideal switch, and is reflected by the switching function (n = a, b, c, for three-phase respectively). U*ia, Uib, Uic* represents the output voltage of three-phase PWM inverter. L and R respectively represent the equivalent inductance and resistance values of the filter inductors and transformers in parallel; C indicates the capacitor value of the inverter DC side; R, L represent the load effects caused by the series converter and two converter switching losses. According to Kirchhoff's law, the state equation of parallel converter voltage, the current equation at DC side, and the voltage equation at DC side can be characterized by formula(11)~(13):

$$(R_1 + L_1 \frac{d}{dt}) \begin{bmatrix} u_{ia} - u_{1a} \\ u_{ib} - u_{1b} \\ u_{ic} - u_{1c} \end{bmatrix} \quad (11)$$

$$i_{dc} = s_a i_{1a} + s_b i_{1b} + s_c i_{1c} \quad (12)$$

$$C \mathrm{d}U_{dc} / \mathrm{d}t = i_{dc} - i_L \quad (13)$$

Where, *Sn=1* (The above bridge turn) or *Sn=− 1* (The below bridge turn). Considering the three-phase equilibrium, the static three-phase coordinates are transferred to rotary two-phase coordinates according to the principle that voltage is constant before and after transformation. Define the three-phase voltage *U ia* ,*U ib* and *U ic* .Synthetic vector is d-axis, the d-q coordinate equation are [9]:

$$\begin{cases} L_1 \dfrac{di_{1d}}{dt} = -R_1 i_{1d} + \omega L_1 i_{1q} + u_{id} - u_{1d} \\ L_1 \dfrac{di_{1q}}{dt} = -R_1 i_{1q} - \omega L_1 i_{1d} + u_{iq} - u_{1q} \end{cases} \quad (14)$$

$$i_{dc} = \frac{3}{2}(s_d i_{1d} + s_q i_{1q}) \quad (15)$$

Shown in Fig.5, the control system formed by the current controller *G id(s)* , *G iq(s)* ,capacitor voltage controller *G u(s)* , current feedback controller *G if(s)*, and voltage controller with current compensation. Fig.6 shows that, d-axis current controller *G id(s)* and q-axis current controller *Giq(s)* all use PI control. They will be unified marked as *G iq(s)* for they are completely similar to each other on the signal path,.

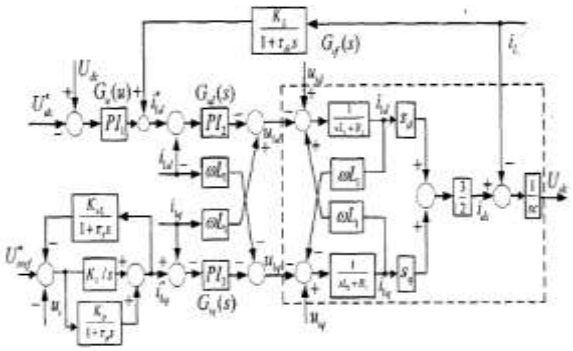

Fig.5 Double loop decoupling control system of shunt converter in d-q synchronous rotating coordinate system

The d-axis component of the output voltage from parallel converter is used to adjust DC bus voltage, and the load current *L i* is introduced in the control system as a feed forward control component. The outer loop voltage and control component constitute the d-axis control system together to adjust the d-axis voltage, and reduce the burden of DC bus voltage PI regulator *G u(s)* .It can also faster the response of PI regulator, and reduce the dynamic process of DC voltage's fluctuations in order to improve system stability. The output of voltage regulator *G u(s)* and the feed forward load current *G if (s)* are the command values of d-axis current, in which the capacitor voltage controller *G u(s)* and inner current control system *G id(s)* are based on the traditional PI controller. The q-axis component of the output voltage is used to regulate the incoming end voltage of the UPFC. The outer loop voltage uses a current-compensated voltage control, it allows the incoming end voltage to have a certain fluctuation when reactive power changes. There is a certain amplitude of the fluctuations. In the same condition, the output current of parallel converter is smaller than the fixed value control, and it's dynamic response time will be also smaller. Voltage control is composed of the PI regulator and a factor. *G iq(s)* uses a traditional inner current PI regulator. Slope is achieved by the current feedback. To improve the stability of control system, the current feedback link uses inertia ratio Ks/ (1 +τ *s)*. Automatic voltage regulation strategy allows a node to have a certain amplitude of voltage fluctuations.

When the node voltage is below the rated value, UPFC shunt converter should output capacitive reactive current, and when the node voltage is higher than the rated value, the output is inductive reactive current. So it can make a better redundancy in the control system.

3.3 Design of series converter controller

The circuit of serial converter is shown in Fig.6. In the figure, *Sa1, Sa2, Sb1, Sb2, Sc1, Sc2* represent switches of each phase leg. *L2* represents the filter inductance of each phase. *R2* represents the internal resistance of filter inductance per phase leg and voltage loss caused by the above and below bridges which interlock the dead zone. R*loss* represents the converter losses. *C2* represents the output filter capacitor. *Cdc* represents the DC bus filter capacitor.

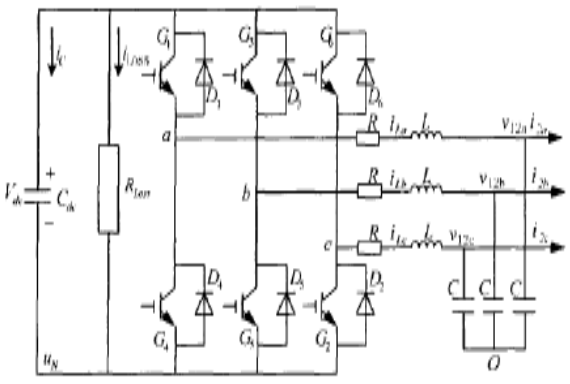

Fig.6 Series converter circuit model of UPFC

The following lists the circuit equations in d-q coordinates:

IJERT

$$\begin{cases} L_2 \dfrac{di_{Ld}}{dt} = -R_2 i_{1d} + \omega L_2 i_{Lq} - v_{12}d + S_d V_{dc} \\ L_2 \dfrac{di_{Lq}}{dt} = -R_2 i_{Lq} - \omega L_2 i_{Ld} - v_{12d} + S_q V_{dc} \end{cases} \quad (18)$$

$$\begin{cases} C_2 \dfrac{dv_{12d}}{dt} = \omega C_2 v_{12q} + i_{Ld} - i_{2d} \\ C_2 \dfrac{dv_{12q}}{dt} = -\omega C_2 v_{12d} + i_{Lq} - i_{2q} \end{cases} \quad (19)$$

This article uses a double loop control based on the output voltage of series converter and output current of filter inductor. It introduces the d-q axis voltage and current state in the two-phase rotating d-q coordinates. Through real-time cross-feedback decoupling matrix, it achieves a decoupling process between the d-q axis. Decoupling control block diagram is shown in Fig.9. UPFC can achieve power grid control through direct controlling of V12d and V12q.

Fig.7 shows that the given voltage signals

*V*12*d** and *V*12*q** are compared with output voltage feedback signals *V*12*d* and *V*12*q* to get the voltage error. Through the voltage regulator, the given inductor current signal *i*1*d** and i1q* are generated. They are compared with inductor current feedback signal to get the current error signal. Then through the current regulator controller, the controlling quantity *Sd* , *Sq* are formed. Feed forward quantities i2d, i2q, v12d, v12q are used to reduce adjusting range. They can also improve performance against load disturbance, and offset the impact of external disturbance on the control system. The voltage loop and current loop introduce the cross-decoupled amount to achieve the independent voltage and current control in the d-q axis.

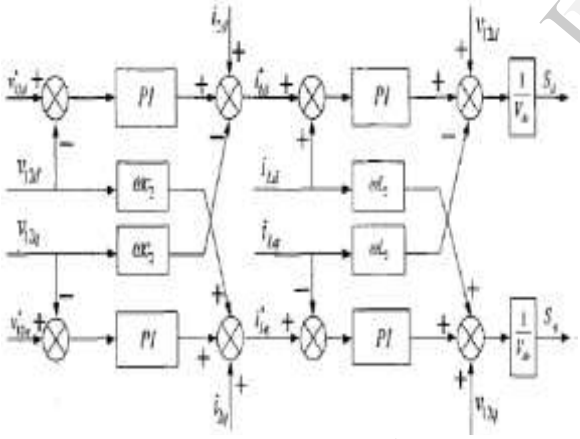

Fig.7 Double loop decoupling control system of series converter in d-q synchronous rotating coordinate system

4. COMPARISON OF PI AND FUZZY CONTROLLER

In this section the behavior of the two current controllers will be compared based on the dynamic response.

4.1 PI Controller

When PI based controller is used, the dc link voltage is sensed at regular intervals and is compared with a reference value. The error signal thus derived is processed in a PI controller [12]. A limit is put on the output of the controller to ensure that the shunt active power filter supplies active power of the load through the series active power filter. The STATCOM model in UPFC is connected in shunt with transmission line using step down transformer. The voltage can be regulated to improve the voltage stability of the power system. Thus the main function of the STATCOM is to regulate key bus voltage magnitude by dynamically absorbing or generating power to the ac transmission line [10].

Simulation diagram of Shunt control block diagram by using PI controller is shown in Fig.8

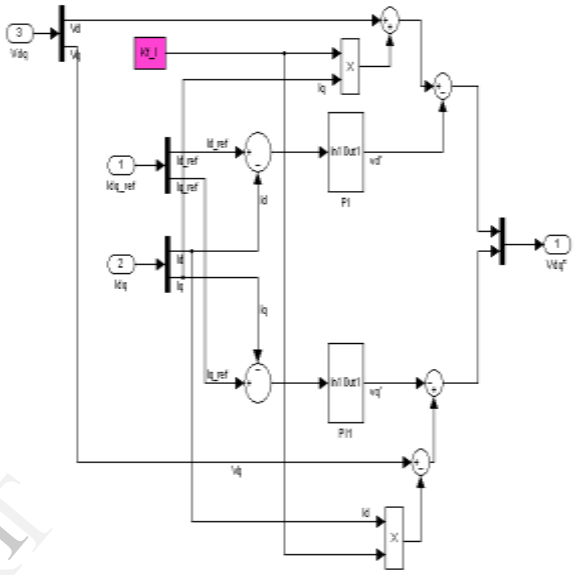

Fig.8 Simulink diagram of Shunt control block diagram by using PI controller

4.2 By comparing PI and Fuzzy Logic Controller (FLC)

The advantages of fuzzy logic controllers over conventional PI controllers are that they [13],

- Do not need an accurate mathematical model,
- Can work with imprecise inputs and
- Can handle Non-linearity's and are more robust than conventional PI controllers.

Fuzzy inference is the process of formulating the mapping from a given input to an output using fuzzy logic. The mapping then provides a basis, from which decisions can be made. The process of fuzzy inference involves membership functions, fuzzy logic operators and if-then rules. Two types of fuzzy inference systems that can be implemented in the Fuzzy Logic Toolbox are,

- Mamdani type and
- Sugeno type

The Mamdani type of fuzzy controller used for the control of gives better results compared with the PI controller. Further, all the coefficients have to be optimized to get better performance than the conventional PI controller. This increases the complexity of the controller. Hence, this demands large computational time. As a result, it may not be useful for real time applications with small sampling time. On the other hand, the fuzzy controller may have an edge over the Mamdani type fuzzy controller in the following features:

- numbers of fuzzy sets used for input Fuzzification,
- number of rules to be used,

IJERT

- number of coefficients to be optimized and
- Computation time.

it is shown that the fuzzy logic controller has improved the dynamic response of the system [11].

4.3 Basic Fuzzy Algorithm

In a fuzzy controller as shown in Figure 9 the control action is determined from the evaluation of simple linguistic rules. The development of the rules requires a thorough understanding of the process to be controlled but it does not require a mathematical model of the system [14].

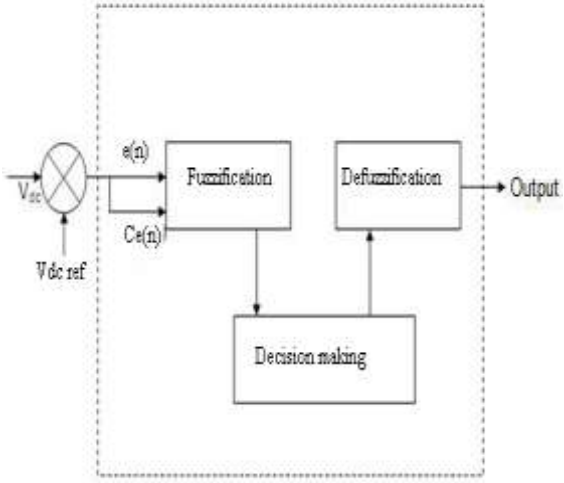

Fig.9 Structure of Fuzzy Logic Controller

A fuzzy controller consists of four stages, namely fuzzification, knowledge base, fuzzy inference mechanisms and defuzzification. The knowledge base is composed of a data base and a rule base, and is designed to obtain good dynamic responses under uncertainty in process parameters and external disturbances. The data base, consisting of input and output membership functions, provides information for appropriate Fuzzification operations, the inference mechanism and defuzzification. The inference mechanism uses a collection of linguistic rules to convert the input conditions into a fuzzified output. Finally, defuzzification is used to convert the fuzzy outputs. In order to implement the control algorithm of Fuzzy Logic Controller, the conventional PI controller is replaced by a fuzzy controller where in the optimum value of fuzzy gain (K) is calculated by a fuzzy inference system, which receives as inputs the slope of D.C. average bus voltage and D.C. voltage error. Both quantities (error and slope of DC voltage) are normalized by suitable values. Thus, each range is from -1 to 1 and normalized to unity. The value of K is chosen to be near unity. To characterize this fuzzy controller, five sets each respective to the error and slope inputs are chosen. The output is defined by five sets. The linguistic rules for the fuzzy logic controller are chosen. These fuzzy rules, used in the object to maintain the K gain not too far from unity, are shown in Table 1. The error 'e' and the change of error 'ce' are used as numerical variables from the real system. To convert these numerical variables into linguistic variables, the following five fuzzy sets are used: NB (negative big), NS (negative small), ZE (zero), PS (positive small) and PB (positive big). The fuzzy controller is characterized as follows: Five fuzzy sets for each input and output are of,

- Triangular membership functions for simplicity,
- Fuzzification using continuous universe of discourse,
- Implication using Sugeno type inference system and
- Defuzzification using the weighted average method.

4.4 Design of Control Rules

The fuzzy control rule design involves defining rules that relate the input variables to the output model properties as the FLC is independent of the system model. The design is mainly based on the intuitive feeling and experience of the process. The control rules are formed by using Table 1. Based on this, the elements of the rule table are obtained from an understanding of the filter behavior and modified by the simulation performance [14-15].

Table1. Fuzzy Rules

Change In Error	Error						
	NB	**NM**	**NS**	**Z**	**PS**	**PM**	**PB**
NB	PB	PB	PB	PM	PM	PS	Z
NM	PB	PB	PM	PM	PS	Z	Z
NS	PB	PM	PS	PS	Z	NM	NB
Z	PB	PM	PS	Z	NS	NM	NB
PS	PM	PS	Z	NS	NM	NB	NB
PM	PS	Z	NS	NM	NM	NB	NB
PB	Z	NS	NM	NM	NB	NB	NB

IJERT

4.5 Fuzzy GUI Tools

There are five primary GUI tools for building, editing and observing fuzzy inference systems in the Fuzzy Logic Toolbox namely,

- The Fuzzy Inference Systems or FIS Editor,
- The membership Function Editor,
- The Rule Editor,
- The Rule Viewer and
- The Surface Viewer.

4.6 FIS Editor

The FIS Editor displays general information about a fuzzy inference system as shown in Fig.10 the FIS Editor handles the high level issues for the system, how many input and output variables are used in the system and their names. The Fuzzy Logic Toolbox does not limit the number of inputs. If the number of inputs is too large or the number of membership functions is too big, then it may also be difficult to analyze the FIS using the other GUI tools.

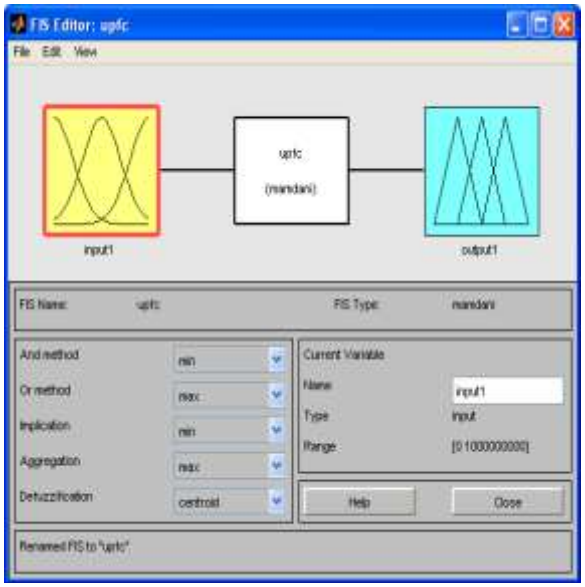

Fig.10 FIS Editor

4.7 Membership Function Editor

The Membership Function Editor tool is used to edit all of the membership functions associated with all of the input and output variables for the entire fuzzy inference system as in Fig.11 & Fig.12.

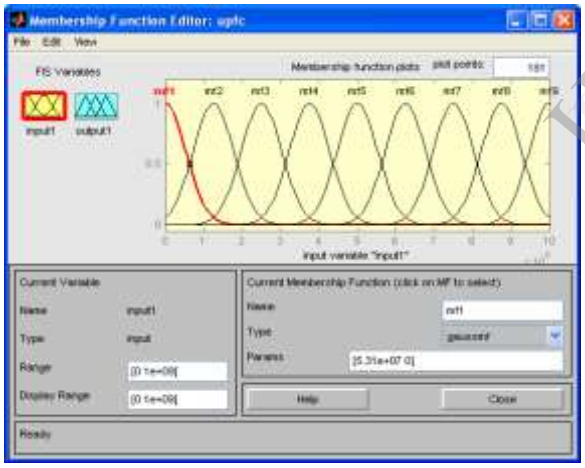

Fig.11 input variable

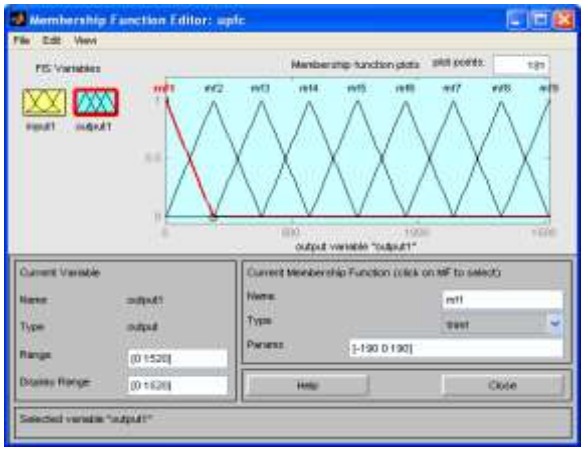

Fig.12 output variable

4.8 Rule Editor

Based on the descriptions of the input and output variables defined with the FIS Editor, the Rule Editor allows to construct the rule statements automatically, by clicking on and selecting one item in each input variable box, one item in each output box and one connection item as in Fig.13 Choosing none as one of the variable qualities will exclude that variable from a given rule. Choosing not under any variable name will negate the associated quality. Rules may be changed, deleted or added by clicking on the appropriate button.

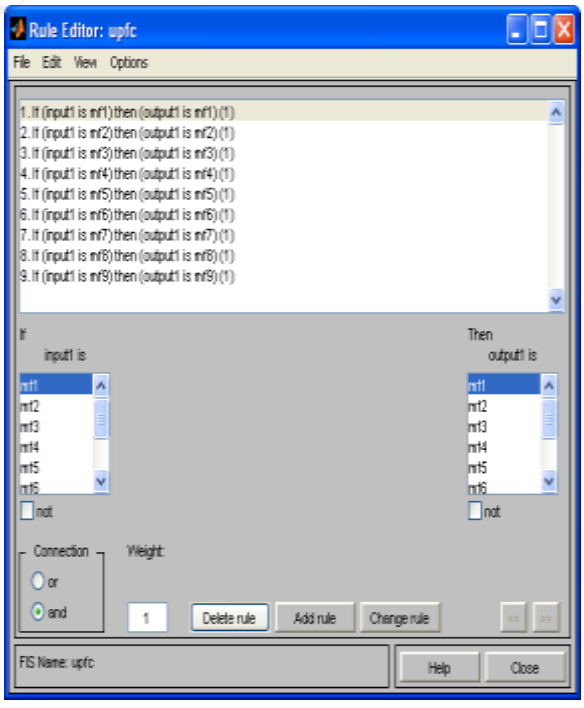

Fig.13 Rule Editor

4.9 Rule Viewer

The Rule Viewer displays a road map of the whole fuzzy inference process as in Fig.14 the three small plots across the top of the figure represent the antecedent and consequent of the first rule. Each rule is a row of plots and

IJERT

each column is a variable. The first two columns of the plots show the membership functions referenced by the antecedent, or the if-part of each rule. The third column of plots shows the membership functions referenced by the consequent, or the then-part of each rule. The Rule Viewer allows interpreting the entire fuzzy inference process at once. The Rule Viewer also shows how the shape of certain membership functions influences the overall result.

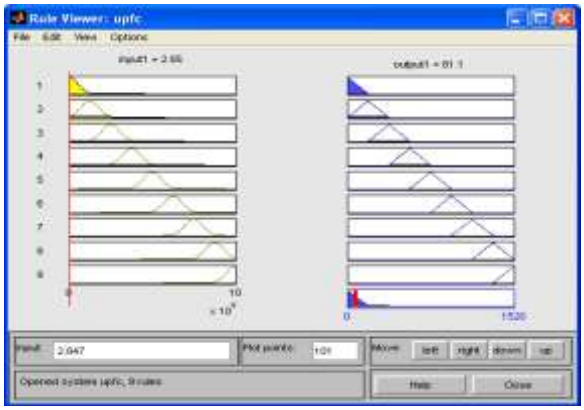

Fig.14 Rule Viewer

The Fuzzy control is basically a nonlinear and adaptive in nature, giving the robust performance in the cases where in the effects of parameter variation of controller is present. It is claimed that the Fuzzy logic controller yields [14, 15] the results which are superior to those obtained with the conventional PI controllers.

Fig.15 The Shunt control block diagram by using Fuzzy Logic Controller in Matlab/Simulink, Shunt inverter is able to reduce the harmonics from entering into the system

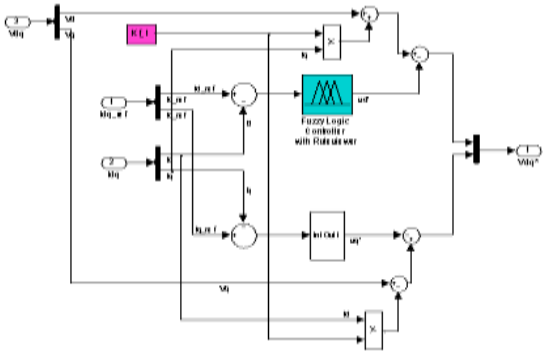

Fig.15 Simulink diagram of Shunt control block diagram by using FLC controller

5. SIMULATION

A. System's main circuit model

A 500KV/230KV transmission system is shown in Fig.16. Main circuit is ring structure, including two large PV power plant (PV plantl, PV plant2), 5 buses (B1~B5), three lines (1 L , 2 L , 3 L), and two 500kV/230kV transformers (*r*1 *T* , *r* 2 *T*) connected to the 230kV transmission lines. PV plantl generates active power 50MW, PV plant2 generates active power 100MW.They all transmit power to the equivalent 15000MVA short-circuit capacity which is connected to the bus B5 and 20MW load which is connected to the bus B3.UPFC is installed at the end of transmission line L2, which is used to control not only voltage on the connected node, but also active and reactive power on the bus B3

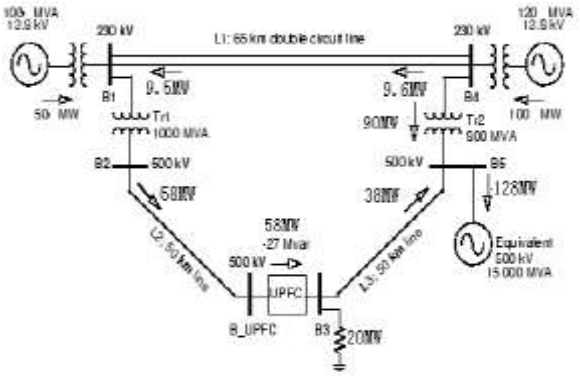

Fig.16 500 KV / 230 KV transmission system

B.Simulink Model

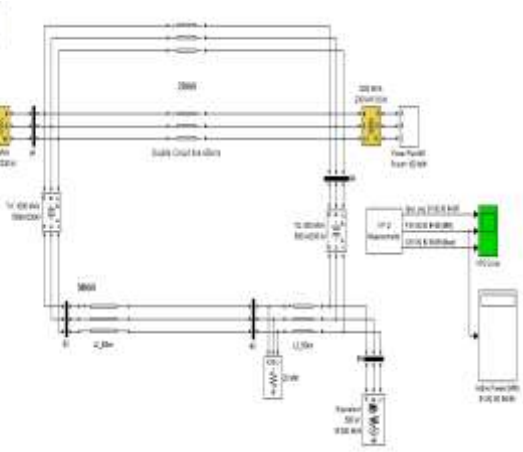

Fig.17 Simulink diagram with out UPFC System

TABLE.II Shows simulated performance of without UPFC measurements ratings

Buses	Voltage(p.u)	Active Power (M.W)	Reactive power (MVAR)
B1	0.9965	-497	2.807
B2	0.9993	588.8	-63.27
B3	0.9995	587	-27.79
B4	0.9925	898.7	26.89
B5	0.9977	1279	-106.4

IJERT

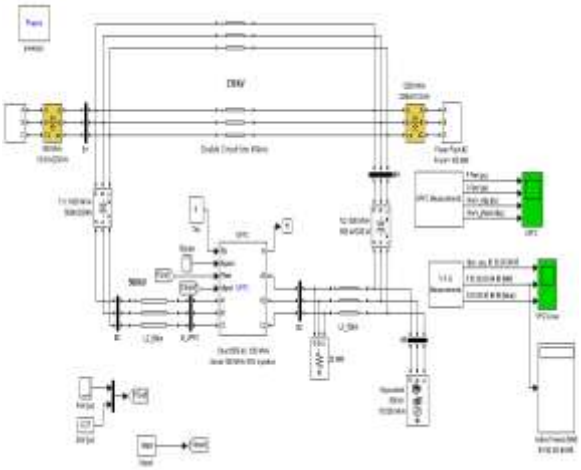

Fig.18 Over all Simulink diagram UPFC System

TABLE.III Shows simulated performance of UPFC with PI Controller measurements ratings

Buses	Voltage(p.u)	Active Power (M.W)	Reactive power (MVAR)
B1	0.9967	-497	4.072
B2	1.002	689.7	-94.05
B3	1.001	687	-27
B4	0.9942	796	15.57
B5	0.9989	1277	-89.32

TABLE.IV Shows simulated performance of UPFC with Fuzzy Controller measurements ratings

Buses	Voltage(p.u)	Active Power (M.W)	Reactive power (MVAR)
B1	0.9812	-496.9	-115.9
B2	0.9663	571	80.46
B3	0.9611	555.1	-311.7
B4	0.9843	916.4	79.02
B5	0.9804	1280	-357.4

B. Results For Upfc Simulation

After establishing a simulation model of UPFC with PI & Fuzzy Controller, regulative characteristics of UPFC to control power flow on the case of steady-state are analyzed. Considering the accidental failure factors of the actual operation, it should be assumed the output power of photovoltaic power plant to be a variety of mutations caused by solar irradiance mutations. In order to verify the ability of UPFC to control the power flow and maintain the node voltage amplitude changeless, the simulation and analysis are as follows.

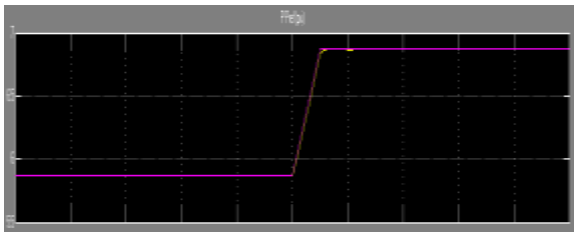

Fig.(a) active power curve and the reference value

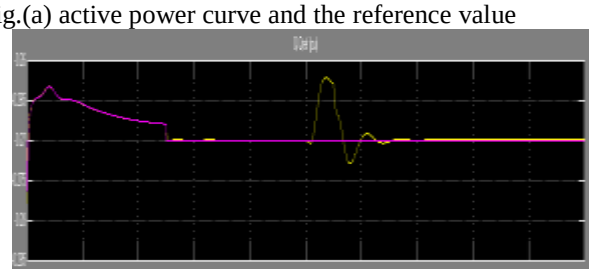

Fig.(b) reactive power curve and the reference value

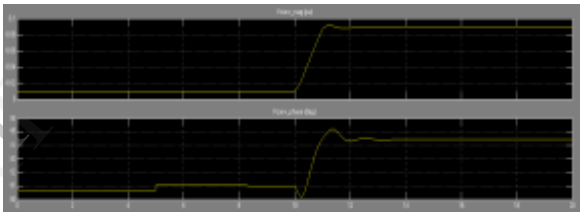

Fig.(c) the changes of voltage *Um* and reference value Uref

Fig.19 UPFC with PI controller active power and reactive power and their reference values

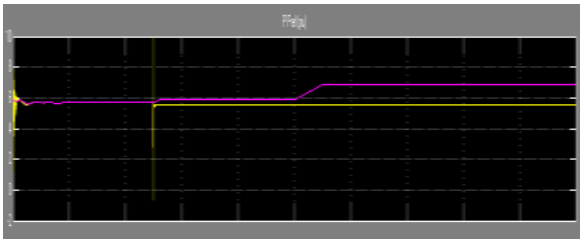

Fig.(a) active power curve and the reference value

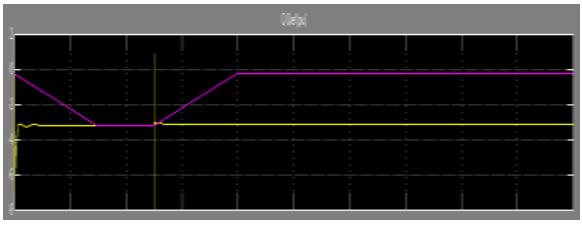

Fig.(b) reactive power curve and the reference value

IJERT

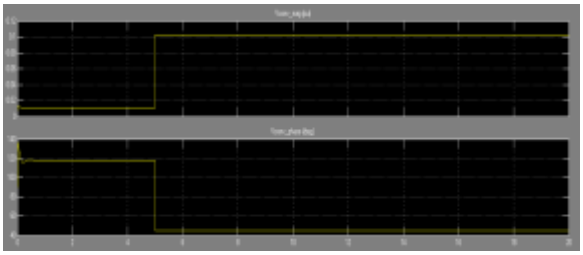

Fig.20 UPFC with PI controller active power and reactive power and their reference values

Fig.19 (a) & Fig.20 (a) shows the active power curve and the reference value. Fig.19 (b) & Fig.20(b) shows the reactive power curve and the reference value. The solid line is the set point while dotted line is the measured value. It can be seen in the 10s that, when the active power set point changes, the measured value of active power is essentially the same, and reactive power measured value can be well consistent with the set value after having experienced volatility.

Fig.19(c) & Fig.20(c) shows the changes of voltage Um and reference value Uref at the access point of UPFC. In the figure, the solid line is the reference value of UPFC voltage Um at the access point. Dotted line shows the UPFC voltage Um at access point. It can be seen that UPFC can control the terminal voltage at the incoming end, makes the voltage fluctuation very small when the power flow changes, and maintain system voltage stability.

Fig.21& Fig.22 shows the system bus voltage, active power and reactive power of PI & Fuzzy controller. Starting from the horizontal 0s, from top to bottom are respectively buses B1, B2, B3, B4, B5. It can be seen that UPFC can quickly control the transmission line active and reactive power and bus voltage. It has a good power flow control functions.

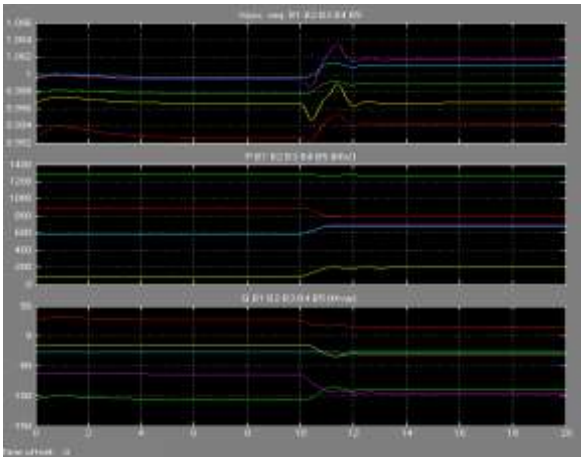

Fig.21 Bus voltage, active power and reactive power in the UPFC system with PI Controller

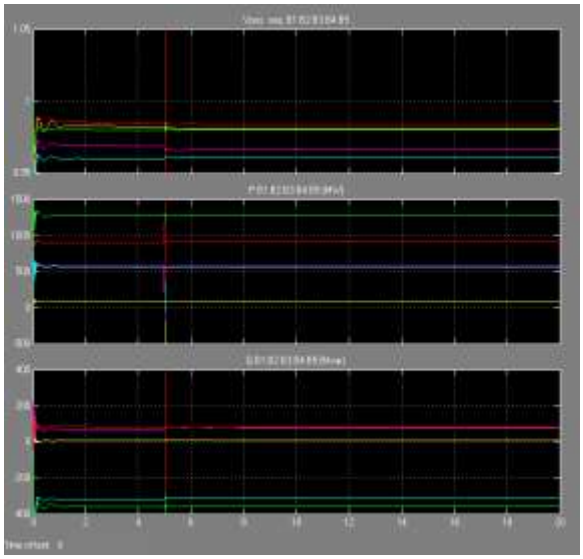

Fig.22 Bus voltage, active power and reactive power in the UPFC system with Fuzzy controller

From the simulation results, it can be concluded that when the set point of active power mutated, the UPFC system as compare to PI the Fuzzy can quickly respond to changes as well as improving power flow. Line active power, reactive power and the access point voltage are able to fast-track set point changes. By changing the inverter, the amplitude and phase angle of output voltage can be obtained. It can ensure that UPFC system as compare to PI the Fuzzy can respond quickly to requirements for adjusting the system's power flow. UPFC achieves effective regulation of the power flow, to ensure the safety of the system.

6. CONCLUSION

UPFC System with PI & Fuzzy control has been the most fully featured device of all FACTS devices so far. It mainly achieves real-time control and dynamic compensation in AC transmission systems. It can adjust the power flow of power system flexibly, keep frequency constant on the side of transmission line, and adjust the voltage and phase of the line. UPFC can provide full dynamic control for transmission line parameters such as voltage, line impedance and phase angle. It is able to control the active and reactive power and bus voltage on the transmission line quickly. It can reduce reactive power exchange between power system and photovoltaic power plant. By comparing PI & Fuzzy It improves both the delivery limits of active power from the PV power plant and power system's stability and security.

REFERENCES

1. Martins C, Demont D. Photovoltaic energy processing for utility connected system[C].The 27th Annual Conference of the IEEE on Industrial Electronics Society, Denver, USA, 2001, 3: 1965-1969.
2. Maryam Hashemi. Using UPFC in order to control power flow[C]. IEEE International Conference on Industrial Technology, 2006, 2: 1486-1491.

IJERT

3. Singh S N, Erlieh I. Locating unified power flow controller for enhancing power system load ability[C]. International Conference on Future Power System, 2005, 1: 16-18.
4. Hingorani N G□Flexible AC transmission [J]. IEEE Spectrum, 1993, 30(4): 40-45.
5. Edris A. FACTS Technology development: an update [J]. IEEE Power Engineering Review, 2000, 0(3): 4-9.
6. J.M.A.Myrzik, M .Calais. String and module integrated inverters for single-phase grid connected photovoltaic systems-A review[C]. IEEE Bologna Power Tech Conference, Bologna, Italy, 2003,2:156-163.
7. Zhang Guorong, Zhang Tieliang, Ding Ming, et al. Combined control of active power filter and PV connected generation [J]. Automation of Electric Power Systems, 2007, 31(8): 61-66.
8. Chen Weimin, Chen Guocheng, Cui Kaiyong, et al. Running control of grid-connected dispersed generation systems in islanding situation[J]. Automation of Electric Power Systems, 2008, 32(9): 89-91.
9. Naik R, Mohan N, Rogers M, et al. A novel grid interface, optimized for utility-scale applications of photovoltaic, wind-electric, and fuel-cell systems [J]. IEEE Trans on Power Delivery, 2005, 10(4): 1920-1926.
10. C.C. Lee. (1990). Fuzzy logic in control systems: fuzzy logic controller, Parts I and II, IEEE Trans. On Systems, Man and Cybernetics, SMC-20, pp. 404-435.
11. Jamshidi, M., Vadiee, N., Ross, T.J.: Fuzzy logic and control: software and hardware applications, 1993, (Prentice-Hall), p. 51-85
12. Lee, C.C.: `Fuzzy logic in control systems: fuzzy logic controller – part Iand part II', IEEE Trans., 1990, (2), p. 404-435
13. Hao Ying, "Fuzzy Control and Modeling: Analytical Foundations and Applications, IEEE Press Series on Biomedical Engineering, Series Editor: Metin Akay, New York, 2000.
14. S. Limyingcharoen , U. D. Annakkage and N. C. Pahalawaththa "Fuzzy logic based unified power flow controllers for transient stability improvement", IEE proc-Gener *Transm. Distrib.*, vol. 145, no. 3, pp.225 -232 1998

IJERT